Bioprinting 35 (2023) e00302

Contents lists available at ScienceDirect

Bioprinting

journal homepage: www.sciencedirect.com/journal/bioprinting

Degradation assessment of Mg-Incorporated 3D printed PLA scaffolds for biomedical applications

Fawad Ali [a,*], Sumama N. Kalva [a], Kamal H. Mroue [b], Kripa S. Keyan [a], Yongfeng Tong [b], Omar M. Khan [a], Muammer Koç [a]

[a] Division of Sustainable Development, College of Science and Engineering, Hamad Bin Khalifa University, Qatar Foundation, Doha, Qatar
[b] Core Laboratories, Hamad Bin Khalifa University, Qatar Foundation, Doha, Qatar

ARTICLE INFO

Keywords:
Additive manufacturing
3D printing
PLA/Mg composite
Biodegradation

ABSTRACT

Polylactic acid (PLA)/Magnesium (Mg)-based composites exhibit great potential for applications in bone regeneration and tissue engineering. PLA is a biodegradable and biocompatible polymer, that has the ability to be easily shaped into diverse structures like scaffolds, films, and fibers. However, its inherent low biodegradability limits its applicability for tissue engineering. On the other hand, magnesium, a biocompatible metal known for its good biodegradability and osteoconductivity, is well-suited for bone tissue engineering. In this study, we fabricated and characterized a composite material of Mg/PLA with 5, 10, and 15 wt%Mg alloy (AZ61), which was subsequently 3D printed. The incorporation of Mg particles into PLA matrix offers a solution to overcome the low biodegradation limitations typically associated with the PLA. Moreover, it helps counteract the negative consequences related to the rapid degradation of Mg, such as alkalinization and excessive release of H_2. Additionally, the change in pH values and changes in mass during *in vitro* degradation indicated that the addition of Mg effectively counteracted the acidic byproducts generated by PLA. Furthermore, X-Ray photoelectron spectroscopy (XPS) and Fourier transform infrared (FT-IR) spectroscopy were utilized to investigate the degradation of the scaffolds, while thermogravimetric analysis (TGA) and differential scanning calorimetry (DSC) were used to compare and contrast the thermal properties of the composites. Our findings demonstrate that the addition of Mg significantly influences the thermal properties of PLA and notably accelerates its degradation, in addition to its noticeable influence on cell adhesion.

1. Introduction

Polylactic acid (PLA) is a widely used biodegradable and biocompatible polymer in tissue engineering and bone regeneration [1]. It offers versatility in shaping, including scaffolds, films, and fibers [2–6]. To enhance cell growth and differentiation, PLA can be combined with biomaterials like growth factors [7]. PLA scaffolds provide structural support for cell attachment and growth in tissue engineering and bone regeneration [8]. These scaffolds mimic the extracellular matrix, promoting cell growth and organization [9–11]. Over time, PLA scaffolds gradually degrade, allowing the replacement of newly formed tissue or bone [12]. The biodegradability of PLA makes it suitable for medical implants requiring gradual replacement during healing [12–14].

Despite the aforementioned favorable properties, PLA has limitations due to its brittleness [15], making the fabrication of complex and porous scaffolds challenging. It may not be ideal for load-bearing bone replacements. The degradation rate of PLA varies, affecting the control of scaffold degradation and tissue or bone regeneration [11]. It can degrade too quickly, compromising mechanical support, or not quickly enough, resulting in scar tissue formation and construct failure. In contrast, magnesium metal is a naturally occurring element with beneficial effects on bone cells, promoting osteoblast growth and differentiation while inhibiting osteoclast activity [16–18].

Recent studies have demonstrated the potential of using polylactic acid (PLA) and magnesium (Mg) as materials compatible with the human body, particularly for bone regeneration and other medical applications [2,19–21]. The combination of these materials into a composite has shown promising results in enhancing the biocompatibility and biodegradation of PLA, thereby making it more suitable for medical implants and tissue engineering [22]. There are two methods for producing Mg-doped PLA composites: blending Mg with PLA and incorporating Mg into the polymer chain during PLA synthesis [15,18,22,23].

* Corresponding author.
E-mail address: faali2@hbku.edu.qa (F. Ali).

https://doi.org/10.1016/j.bprint.2023.e00302
Received 28 July 2023; Received in revised form 8 August 2023; Accepted 10 August 2023
Available online 11 August 2023

Table 1
Compositions of synthesized PLA/Mg composites.

Material	Polymer matrix (w%)	
	PLA	Mg
PLA	100	00
PLA/5 Mg	95	05
PLA/10 Mg	90	10
PLA/15 Mg	85	15

The amount of Mg, particle size, and distribution within the PLA material, can significantly influence their characteristics [24]. In vitro studies have demonstrated that Mg-doped PLA composites facilitate the attachment, proliferation, and differentiation of various bone cell types, including osteoblasts and osteocytes [25]. The biocompatibility, mechanical properties, and cell proliferation of the composites are influenced by the Mg content [18]. Animal studies have also shown that Mg-doped PLA composites have the ability to promote the formation of new bone tissues [26].

The aim of this research endeavour was to develop a PLA/Mg composite printable by the fused deposition modeling (FDM) printing technique for biomedical applications. To this end, we have produced 3D printed PLA/Mg scaffolds with varying amounts of Mg content, and the effect of Mg concentration on the degradation and thermal properties were investigated using a variety of characterization techniques such as XPS, FT-IR, DSC, and TGA.

2. Materials and methods

2.1. Materials

Polylactic acid (PLA) granules were obtained from Goodfellow Cambridge Limited (England), having a size in the range of 3–5 mm. These granules have a melting point of approximately 170 °C and an average molecular weight of about 68,000 g/mol. The Mg alloy powder (AZ61, 99.95% purity) was supplied by Nanografi Nanotechnology (Turkey) and had an average diameter of 100 μm. To dissolve the PLA, we used chloroform provided by VWR Chemicals, Germany. The chloroform has a boiling point of 59.5–60.5 °C and a density of 1.48 kg/L.

2.2. Solution preparation and filament formation

PLA solution was prepared as proposed previously [20], the PLA solution was prepared by mixing PLA granules with chloroform, creating a solution with a concentration of 20 g/L. The mixture underwent mechanical stirring at 400 rpm for 4 h to ensure thorough blending. To create PLA/Mg composites with varying Mg content (5 wt%, 10 wt%, and 15 wt%, as detailed in Table 1), we added the Mg alloy powder to the chloroform/PLA solution. The stirring continued for 24 h at room temperature, allowing for a uniform dispersion of Mg particles.

Subsequently, the well-mixed solution was poured onto a metal plate and allowed to air-dry for 24 h at room temperature before being peeled from the metal plate. For further enhancement, the PLA/Mg sheets were dried in an oven overnight at 60 °C after the chloroform had evaporated. Once the chloroform had evaporated, we collected the PLA/Mg composites for characterization. To transform these composites into functional filaments, the films underwent shredding and extrusion using the advanced Filabot EX2 system (Filabot, Vermont, VT, USA). The filament-making process involved melting and blending the extruded material at a temperature of 175 °C, passing it through a nozzle with a diameter of 2.75 mm. The resulting filaments were then uniformly shredded into smaller pieces. For consistent distribution of Mg particles throughout the filaments, these shredded pieces were reintroduced into the extruder for a second pass. This step ensured that each filament possessed an even distribution of Mg particles, tailored to different Mg concentrations. These innovative modified filaments, containing distinct levels of Mg, were ready for subsequent investigations and held immense potential for diverse 3D printing applications.

2.3. Characterization

The thermal stability of the PLA/Mg composites was evaluated using Thermogravimetric Analysis (TGA) conducted on a TA SDT 650 instrument. The composites were carefully placed into a ceramic crucible and subjected to a controlled heating process from room temperature to 500 °C at a rate of 10 °C/min, all under a nitrogen atmosphere. From the resulting testing curves, key thermal properties such as the cold crystallization temperature, melting point, and decomposition temperature were determined using Differential Scanning Calorimetry (DSC), alongside the remaining mass percentage at 500 °C from the TGA analysis. To examine the surface morphology of the composites, a Field Emission Scanning Electron Microscope (FE-SEM) operating at an accelerating voltage of 20 kV and a working distance of 9.0 mm was utilized with the imaging conducted on the FEI Quanta650FEG.

Fourier transform infrared (FT-IR) spectroscopy was used to detect the microstructural changes that might occur in the PLA/Mg composites before and after degradation in PBS solution. FT-IR analyses were conducted using a Thermo Scientific Nicolet iS50 FT-IR spectrometer, which was fitted with an attenuated total reflectance (ATR) sampling accessory featuring a diamond crystal plate. Spectra were recorded with 32 scans per sample/background in the spectral range spanning from 4000 to 400 cm^{-1}, with a high spectral resolution of 4 cm-1. Advanced ATR correction was performed on the collected spectra using the OMNIC 9.3 software package. The obtained results were plotted in transmittance mode and normalized to the highest peak intensity for comparison.

The degradation of the 3D printed scaffolds was studied by immersing the PLA/Mg scaffolds in PBS solution with an initial pH value of 7.6 for four weeks. The weight loss and weight gain of the scaffolds were measured after week 2 and week 4, respectively. All the scaffolds' weights were measured before immersion in PBS. The weight gain (solution intake) was measured after removing the samples from PBS and drying them after 2 and 4 weeks, respectively. The weight loss of the scaffolds was measured with subsequent oven drying at 50 °C for 8 h. The scaffold's percentage of weight gain and weight loss (ΔW%) was determined using the following formulas:

$$\Delta W\% = (W_f - W_i)/W_f \times 100\%, \text{ weight gain}$$

$$\Delta W\% = (W_i - W_f)/W_i \times 100\%, \text{ weight loss}$$

where W_i and W_f are the initial and final weights of the dried degraded scaffolds, respectively. Furthermore, the pH value of the immersion medium was measured using a pH meter.

The X-ray photoelectron spectroscopy (XPS) is performed on the PLA and PLA/Mg scaffolds after four weeks of immersion in PBS using a Thermo Fisher Escalab250XI platform with an monochromatic Alkα source(1486.8eV) and a hemisphere analyzer. The overall resolution is estimated to be better than 0.5eV. The Survey spectra are taken with an energy step of 1eV and a pass energy of 100ev while the high resolution is taken with a step of 0.1ev and a pass energy of 20eV. All measurement is conducted in an ultra-high vacuum of 10^{-10} mbar at room temperature. The deconvolution is conducted with a Voigt type profile(GL(30)) after a proper Shirley background subtraction.

2.4. 3D printing of PLA/Mg filaments

The synthesized PLA/Mg composite filaments were successfully 3D printed via FDM (SOVOL-SV02 by SHENZHEN Lian Dian Chuang Technology LTD, Guangdong, China) based printer. Initially, the desired size of the scaffolds was created using SolidWorks software and saved in the Stl format. Next, slicer software was used to divide the designed model into layers, generating G-code instructions for the 3D printer. The printer's head had the ability to move horizontally in the x and y

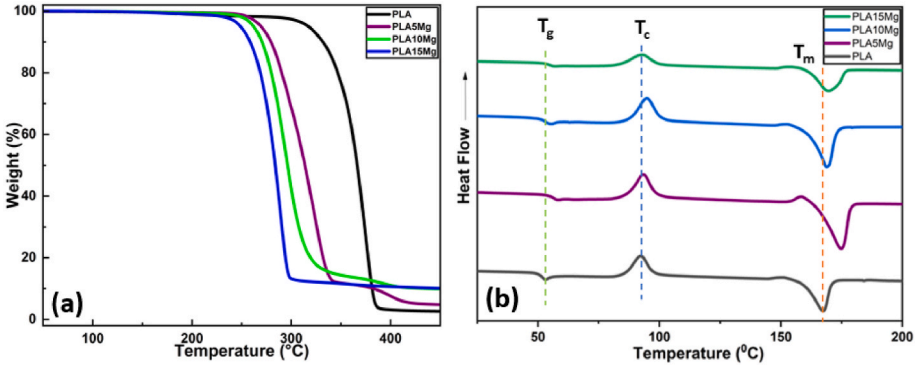

Fig. 1. (a) TGA and (b) DSC results for PLA/Mg composites with varying amounts of Mg, showing the thermal stability and heat flow of PLA as the Mg content.

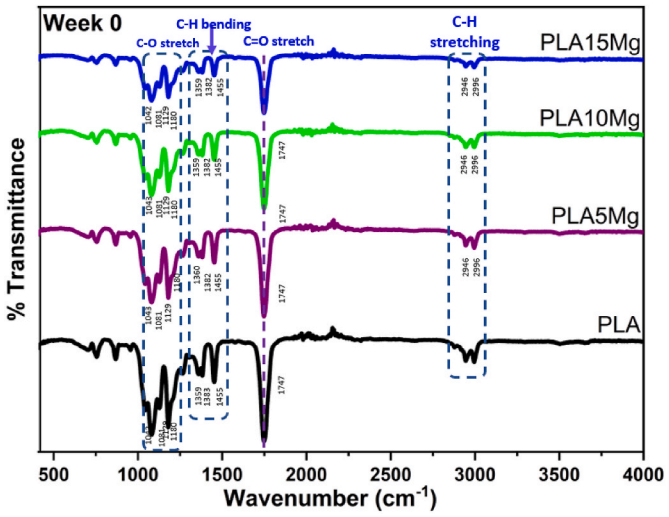

Fig. 2. FT-IR spectra of PLA and PLA/Mg composites with various Mg concentrations (0/5/10/15 wt% Mg).

directions. As the filament passed through the heating region, it rapidly melted, transforming into a liquid polymer that was then extruded onto the printer bed through a nozzle. Once a layer was fully deposited, the printer bed moved downward by the height of a single layer, allowing the printer head to proceed with printing the subsequent layer. This sequential layering process continued until the final layer was completed.

2.5. Cell culturing

An *in vitro* cell study was conducted to examine the behavior of MCF7s, an epithelial cell line, on PLA/Mg scaffolds. The cells were cultured for a period of five days at 37 °C supplemented with 10% fetal bovine serum, 100 U/mL penicillin, and 100 g/mL streptomycin. To prepare the scaffolds for cell seeding, they were first treated with ethanol, allowed to air dry, and then subjected to 20 min of UV sterilization on each side. Following sterilization, the samples were washed with PBS and soaked in culture media overnight before being seeded with MCF7 cells at a density of 3 × 104 cells/sample. This seeding process was performed to study cell attachment.

2.5.1. Cell attachment

To investigate cell attachment on the surfaces of PLA/Mg scaffolds,

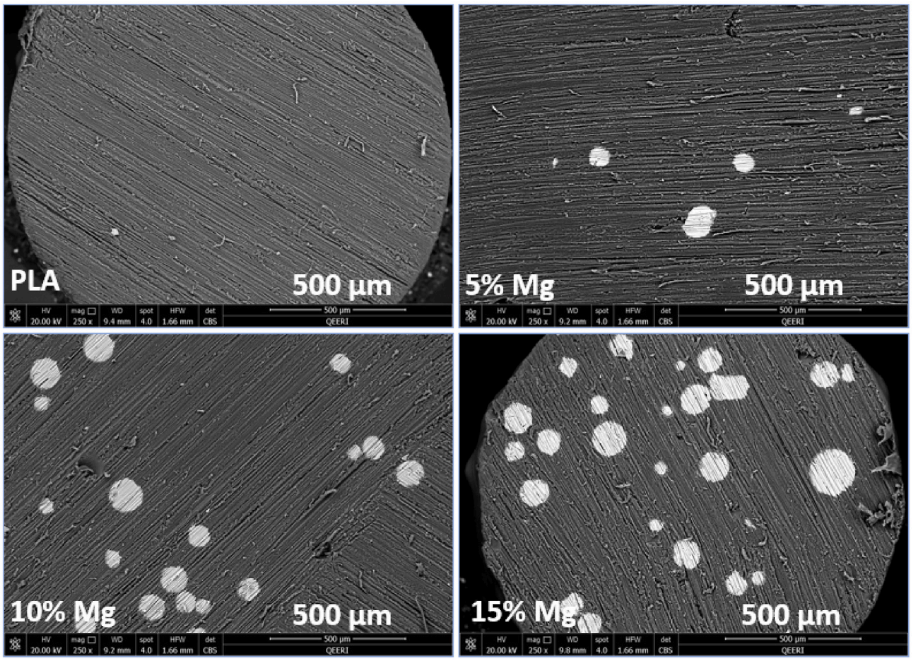

Fig. 3. SEM images of PLA and PLA/Mg composite filaments with various Mg amounts (0, 5, 10 and 15 wt%).

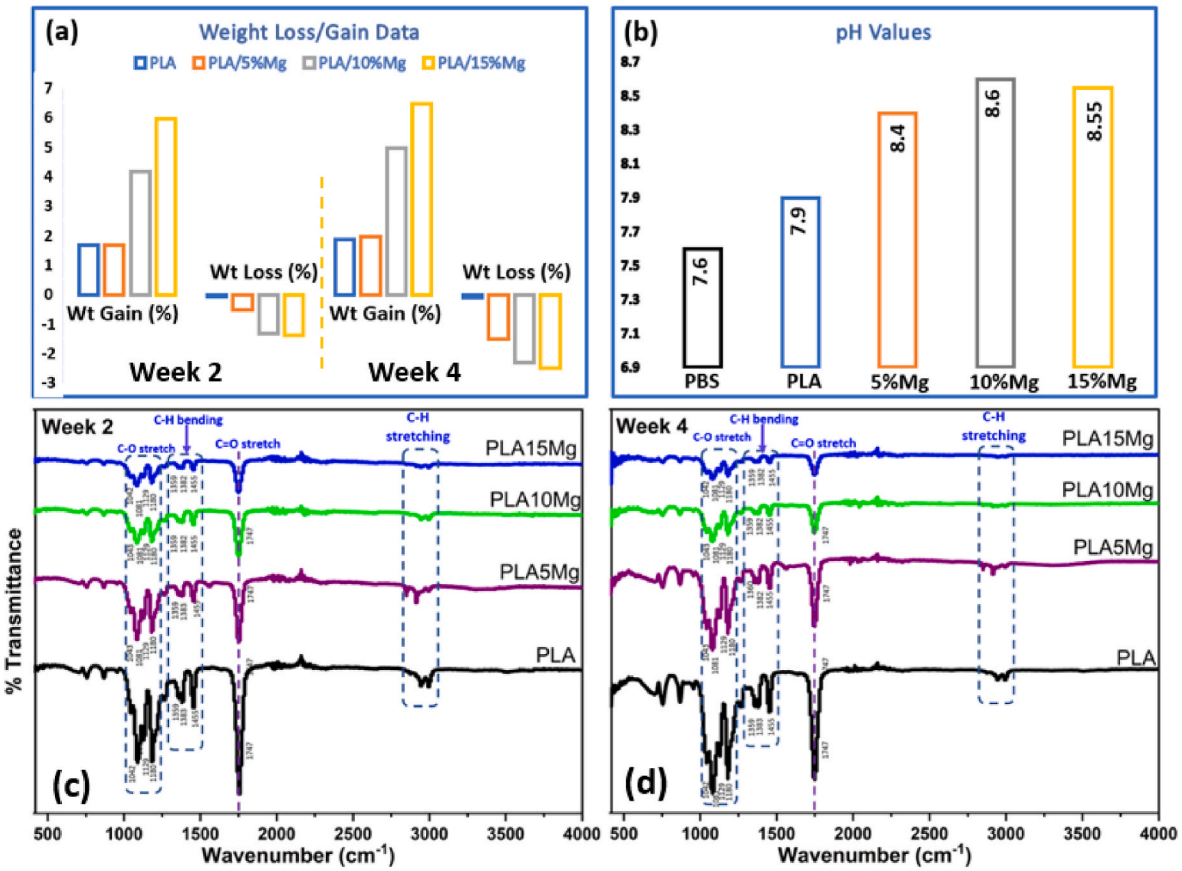

Fig. 4. (a) PLA/Mg scaffolds weight gain and weight loss, (b) pH values of PLA/Mg after immersion in PBS for four weeks, and FTIR results showing the degradation of PLA and PLA/Mg composites in PBS solution dissolved for (c) 2 weeks and (d) 4 weeks.

Table 2
pH values and weight gain and loss of PLA and PLA/Mg scaffolds after immersing in PBS for four weeks.

Materials	pH Values	Week_2		Week_4	
		Wt Gain (%)	Wt Loss (%)	Wt Gain (%)	Wt Loss (%)
PBS	7.6				
PLA	7.9	1.7	0.05	1.9	0.1
PLA/5%Mg	8.4	1.7	0.5	2.0	1.5
PLA/10% Mg	8.6	4.2	1.3	5.0	2.3
PLA/15% Mg	8.55	6.0	1.37	6.5	2.5

scanning electron microscopy (SEM) was employed. After a period of 48 h, the cells were fixed using a 3% glutaraldehyde solution, followed by rinsing in distilled water. Subsequently, the cells were dehydrated using a series of ethanol solutions with increasing concentrations (ranging from 50% to 100% [v/v]). The prepared samples were then coated with a layer of carbon using sputter coating and observed using SEM, specifically the Philips XL30 model.

3. Results and discussion

3.1. Thermogravimetric analysis (TGA)

In order to track the weight change variation of the PLAL/Mg scaffold as a function of temperature or time in a controlled atmosphere, thermogravimetric analysis (TGA) was used. TGA is common technique for determining the thermal properties of a material, such as thermal

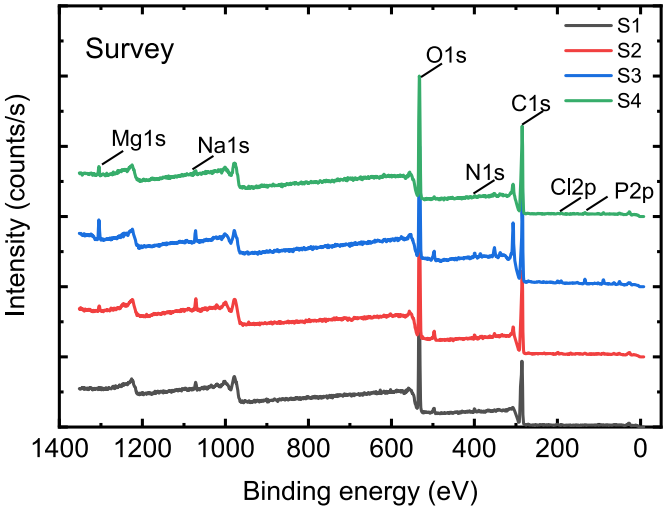

Fig. 5. The XPS survey spectra of the PLA and PLA/Mg scaffolds with 5, 10 and 15% Mg.

Table 3
The atomic ratio (%) of all elements for PLA and PLA/Mg scaffolds.

	Mg1s	P2p	Cl2p	C1s	N1s	O1s	Na1s
PLA	0	0.21	0.36	65.29	1.16	32.13	0.84
5%Mg	0.69	0.38	0.46	65.09	1.23	30.95	1.2
10%Mg	1.76	1.67	0.41	65.40	2.10	27.36	1.06
15%Mg	0.99	1.03	0.15	59.20	0.82	37.13	0.69

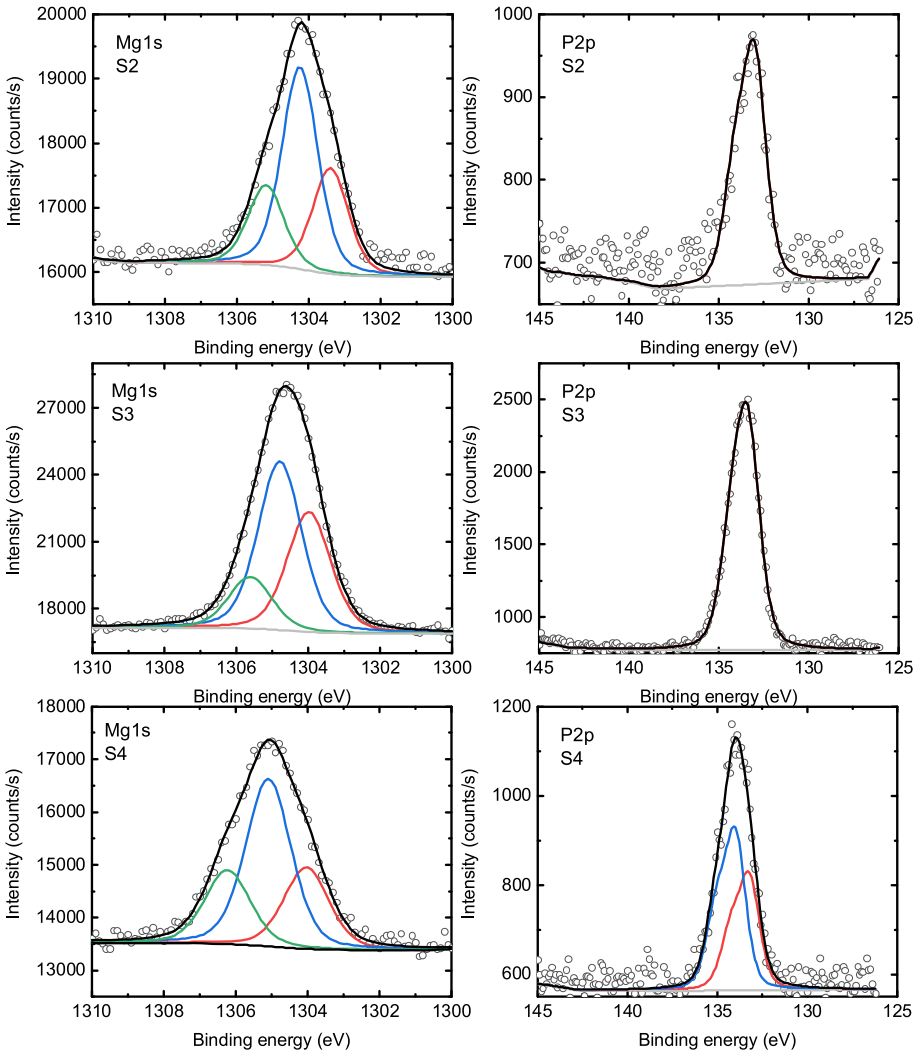

Fig. 6. The deconvolution of Mg1s(left column) and P2p (right column) for the PLA/Mg scaffolds with 5, 10 and 15% Mg. A Voigt type profile is chosen after a proper Shirley background subtraction.

stability, decomposition temperature and the extent of weight loss due to thermal decomposition. When examining polylactic acid (PLA), TGA can help identify the temperature at which degradation initiates and quantify the extent of degradation at different temperatures. In the study mentioned, TGA was used to evaluate how different concentrations of Mg affected the thermal stability of PLA/Mg scaffolds. As shown in Fig. 1a, all samples experienced an initial mass loss after reaching 70 °C, which can be attributed to the evaporation of the solvent. Comparing the pristine PLA with the PLA/Mg composites, it was observed that the thermal degradation behavior differed significantly. The unmodified PLA started to degrade thermally at temperatures between 300 °C and 350 °C, while the PLA/Mg composites exhibited an earlier onset of degradation, occurring between 250 °C and 300 °C. The addition of Mg to the PLA accelerated the breakdown of heat in the composite material, signifying its catalytic effect on the depolymerization reaction of PLA when exposed to elevated temperatures [27,28]. The amount of residual Mg detected at 500 °C aligned with the actual quantity used during the experimental process. Any minor deviations in the values can be attributed to the handling of such small quantities of materials.

3.2. *Differential scanning calorimetry (DSC)*

The thermal properties of PLA and PLA-Mg composites were evaluated using DSC, and the results are reported in Fig. 1b. The characteristics of semi-crystalline PLA, i.e., the glass transition temperature (T_g), crystallization temperature (T_c), and melting temperature (T_m), can be.seen and compared in all the specimens. It can be observed that the T_g of PLA increases with the addition of Mg particles from 53 °C to 57.7 °C with 15 wt% Mg. T_g is dependent on various factors, including intermolecular interaction, chain mobility, and molecular weight. Since the molecular weight of PLA remains constant across all samples, the observed increase in *Tg* (glass transition temperature) can be attributed to the interaction between the polymer chains and Mg particles. This interaction leads to reduced mobility and lubrication of the PLA molecular chains [29]. Additionally, the presence of Mg in the composites suggests that the Mg particles serve as nucleation agents, promoting crystallization. As a result, the crystallization time decreases due to the heterogeneous nucleation effect of these particles [29,30]. The melting temperature for all specimens was approximately 167 °C, with a slight increase to 169.8 °C for the PLA/Mg scaffold containing 15 wt% Mg. Compared to pure PLA, the PLA/Mg composites exhibited higher melting temperatures. However, when the Mg content increased from 0 to 5%, there was a slight decrease in melting temperature. This implies that the incorporation of Mg particles into the PLA matrix has a limited impact on the crystalline structure of PLA.

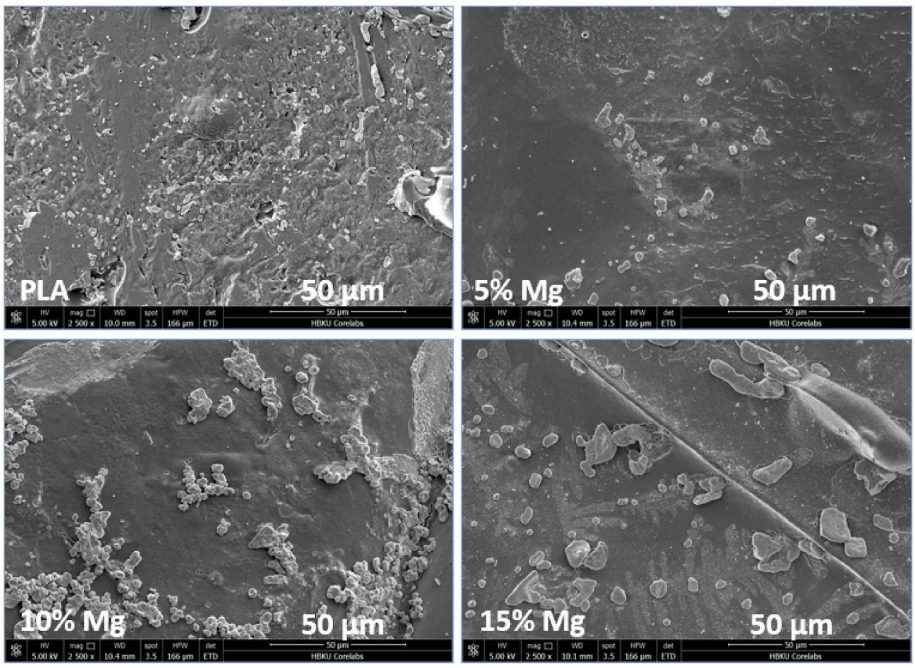

Fig. 7. MCF7 cells attachment to PLA and PLA/Mg scaffolds.

3.3. Fourier transform infrared spectroscopy (FT-IR)

To analyze a PLA/Mg composite using Fourier transform infrared (FT-IR) spectroscopy, the PLA/Mg scaffold is placed in contact with the crystal of the ATR module of an FT-IR spectrometer, and the absorption of IR radiation by the sample is measured over a range of wavelengths. FT-IR spectroscopy is ideally suited for the identification and characterization of polymer materials. As shown in Fig. 2, the FT-IR spectrum of a PLA/Mg composite shows the vibrational bands of the chemical functional groups present in the PLA matrix and the Mg reinforcing particles. The intensity and frequency/position of these bands can be used to quantify the relative amount of each component in the composite and to determine the degree of interaction between the two materials. Slight shifts in the frequency/position of the observed bands and/or variations in relative peak intensities indicate changes in the molecular structure and/or changes in the local environment surrounding the compound under study. The FT-IR spectrum is capable of detecting additional components in the composite, such as additives or impurities. However, in this case, only minor discrepancies between PLA and PLA/Mg composites were observed, indicating that the chemical linkages were comparable and consistent with existing literature [31]. While there is a slight shift in the C–H stretch, overall, there are no significant differences in peak positions, although the peak intensities showed a slight reduction after the incorporation of Mg particles. The intensity of peaks at 2947 cm^{-1}, associated with CH_2 stretching, decreased as the concentration of Mg in the composite increased. This observation supports the idea that there is an interaction between the ester group (R–COOR') in PLA and the chemical groups of the dispersants (–NH–, -NH2, N^{+}). Furthermore, the peak at 1747 cm-1, which is characteristic of PLA and corresponds to the carbonyl bond of the ester group, exhibited reduced intensity as the amount of Mg in the composite increased. This suggests that the composites may be undergoing degradation or interaction with another component.

3.3.1. Scanning electron microscopy (SEM)

A cross-sectional scanning electron microscopy (SEM) study was conducted to investigate the distribution of Mg particles within PLA matrix in PLA/Mg filaments with 5, 10 and 15% of Mg concentration, as shown in Fig. 3. The study aimed to understand how the concentration of Mg affected the spatial arrangement and dispersion of Mg particles in the composite material. As shown in Fig. 3 that Mg is evenly distributed in the filaments. The cross-sectional images show that there is no defects and air gap in the filaments and the Mg incorporation has not introduced any cracks as well. The Mg particles were completely encapsulated within the polymer matrix, ensuring that they were consistently surrounded by a layer of PLA. This distribution of polymer around the particles indicates that the Mg particles serve as nuclei during solvent evaporation in the PLA. The quality of 3D printed scaffolds is significantly influenced by the presence of a uniform Mg distribution and the absence of air gaps and cracks in PLA/Mg filaments. Moreover, the absence of defects contributes to improved printability and process stability during 3D printing, resulting in the accurate reproduction of the scaffold's desired geometry.

3.4. Degradation of PLA/Mg composites

To investigate the influence of Mg content on the degradation of PLA composites, *in vitro* degradation tests were performed using a phosphate-buffered saline solution (PBS). The PLA samples and PLA/Mg composites were immersed in PBS for durations of two and four weeks, after which they were subjected to characterization using FT-IR analysis. After immersing PLA/Mg scaffolds in phosphate buffer saline (PBS) for a duration of 4 weeks, the weight gain and weight loss of the scaffolds were carefully evaluated to understand their degradation behavior and stability in a physiological environment. The interaction between the scaffolds and the PBS solution during the immersion period resulted in changes in their weights and the values are presented in Fig. 4a. As shown in Fig. 4a, the weight of the scaffolds increased with the increasing percentage of Mg alloy in the PLA for both the week 2 and week 4 samples. The scaffolds with 15% Mg retained the highest amount of weight (*i-e*, 6 and 6.5%, for week 2 and week 4, respectively). Similarly, the weight loss followed a similar trend with the increasing amount of Mg in the PLA. As shown in Fig. 4a, the amount of weight loss is not that significant as compared to the literature [32]. This little decrement in weight indicates the accumulation of additional material on the surface of the scaffolds, possibly due to the adsorption of ions or proteins from the PBS solution (the corrosion product deposition on the sacffold's surface). Weight loss was observed in all of the samples, with

noticeable differences among them. Notably, the PLA scaffolds exhibited the lowest weight loss at every time point and demonstrated minimal changes after 4 weeks. In contrast, the PLA/Mg scaffolds experienced significantly higher weight loss compared to the PLA scaffolds, and this weight loss increased proportionally with the addition of Mg; a similar trend has also been reported in the literature [33]. These results strongly suggest that the presence of Mg accelerates the degradation process of the scaffolds. The weight loss reflected the degradation or dissolution of the PLA/Mg scaffolds, indicating their ability to break down and potentially be replaced by new tissues during the tissue regeneration process. The pH values of the solution was measured after four weeks of scaffold's immersion and are presented in Fig. 4b. The obtained results indicated that as the concentration of Mg increased in the scaffolds, the pH values of the immersion medium exhibited a trend towards higher alkalinity. The pH values increased from 7.9 for pure PLA to 8.55 for the PLA/Mg scaffold containing 15% Mg. This suggests that the degradation of PLA/Mg scaffolds led to an increase in the pH of the surrounding environment. The release of Mg ions during the degradation process and the production of $Mg(OH)_2$ might have contributed to this alkalizing effect [33,34]. Table 2 summarises the pH values and weight gain/loss data of the PLA and PLA/Mg scaffolds in PBS for four weeks.

In order to better understand the microstructural changes that might occur in the samples upon immersion in PBS solution, FT-IR measurements were also conducted on the samples to compare and examine degradation caused by immersion in PBS. Fig. 4 (c,d) shows the FT-IR spectra of films with 5, 10, and 15 wt% of Mg particles in PLA. The wide band with considerable width that appears in the degraded films at 3400 cm^{-1} in composites with Mg composition of 10 wt% and beyond is attributed to the carboxylic acid group, indicating the significant degradation of the polymer chain during the composite immersion, which is significantly higher with a higher percentage of Mg in the PLA [20]. The peak at 3000 cm^{-1}, related to the stretching of the OH group caused by PLA hydrolysis, shows a similar trend and completely disappeared for the sample with 10 and 15 wt% Mg after four weeks of immersion in PBS as shown in Fig. 4 (c, d). The most characteristic band of PLA at 1747 cm^{-1}, associated with the carbonyl band and of the ester group, has significantly less intensity for the degraded scaffolds. The PLAband at 1747 cm^{-1} exhibits high sensitivity to changes resulting from polymer degradation or interaction with another component, leading to a reduction in intensity or a downward shift in wavelength. As can be seen for both week 2 and week 4, the peak intensity is significantly reduced for the samples with the increasing concentration of Mg (10 and 15 wt% Mg) [35,36]. Also, the band at 1454 cm^{-1} attributed to the CH_3 group has reduced intensity for the composite having 10 and 15 wt% Mg after four weeks of immersion in PBS. Additionally, the peaks at 2950 and 3000 cm^{-1} disappeared after four weeks of immersion in PBS for the scaffolds with 10 and 15% Mg. This is a clear indication of the interaction between the ester group (R–COOR') from PLA with Mg particles. In conclusion, the Mg addition to PLA has demonstrated a faster degradation of PLA with 10 and 15 wt%, while 5 wt% Mg did not have noticeable effect on the degradation rate of PLA.

3.4.1. XPS study of PLA/Mg scaffolds

To further analyze the degradation of PLA and PLA/Mg scaffolds in PBS, XPS was conducted so analyze the corrosion products deposited on the scaffold surface, and the comparison of the Survey spectra of the samples is shown in Fig. 5. While the signal of Na1s, O1s, C1s, Cl2p, and P2p can be clearly observed in all samples, the Mg1s only exist on the surface of the samples with 0, 5, 10 and 15% Mg defined as S1, S2, S3 and S4, respectively. Their atomic ratio is given in Table 3. The comparison of core levels are given in the supporting information Fig. S1, where the Mg1s present a strong energy shift and variation in profile is also be observed in C1s and O1s for the corresponding samples.

To understand the binding energy shift of Mg1s, we perform the deconvolution of the Mg1s and P2p given in Fig. 6, as shown, the Mg1s can be fitted with 3 components in each sample. The PLA/Mg scaafolds give position of 1303.4eV, 1304.2eV and 1305.2eV, which can be assigned to Mg–O, Mg–OH and Mg-PO_3, respectively. The first component disappear in the samples with 10 and 15%Mg, and instead another component at high BE side of 1305.6eV(PLA10%Mg) or 1306.2eV (PLA15%Mg) is observed, which is a signature of Mg-PO_4 bond. This is also proven by the variation of P2p signal in the right column in Fig. 6. While the samples with 5 and 10%Mg give only one component at around 133eV(P2p3/2) relating to $(PO3)^{n-}$ signal, a new component at 134eV appears for the sample with 15% Mg, which may be assigned to the $(PO4)^{n-}$ structure.

3.5. Cell attachment

Cell attachment is a critical aspect to consider in tissue engineering and regenerative applications. To investigate the cell adheshion to PLA and PLA/Mg composites with 5, 10, and 15%Mg, SEM investigation was conducted and the results are reported in Fig. 7.

Fig. 7 shows that more and more cells are attached to the PLA/Mg scaffolds surface with the increasing Mg concentration in the scaffold. This indicates that these particles were beneficial for the adherence of cells to the scaffold surface. Various factors contribute to the cell's adhesion on the scaffold surface, including surface roughness and hydrophilicity [37]. In line with the published reports that Mg incorporation into PLA enhances the surface hydrophilicity [38], the large number of cell attachments to the scaffolds with 10 and 15% Mg as compared to pure PLA might be attributed to the increased hydrophilicity.

4. Conclusions

In this study, we successfully 3D-printed PLA/Mg scaffolds using FDM technique. The effect of Mg incorporation on the PLA/Mg scaffolds thermal behavior, degradation, and cell attachment was studied. The incorporation of Mg particles played an essential role in enhancing the degradation rate, and changing the thermal behavior of PLA/Mg composite scaffolds. Mg incorporation also had a positive impact on the cell attachment to the PLA/Mg scaffolds. The FTIR results showed that there was a significant increase in the degradation of PLA with 10 and 15 wt% Mg particles as the peek intensities for these scaffolds significantly reduced after immersing in PBS for four weeks. These results were further confirmed by XPS. Mg incorporation also changed the glass transition temperature and melting point of the PLA. Overall, the inclusion of Mg is crucial for addressing various challenges encountered in PLA, including hydrophilicity, degradation rate, and thermal properties.

CRediT authorship contribution statement

Fawad Ali: Conceptualization, Methodology, Experiment, Formal analysis, Writing – original draft, preparation, Validation. **Sumama N. Kalva:** Experiment, review Manuscript. **Kamal H. Mroue:** FT-IR, Investigation. **Kripa S. Keyan:** Cell culturing. **Yongfeng Tong:** XPS analysis. **Omar M. Khan:** Review. **Muammer Koç:** Funding and Review.

Declaration of competing interest

The authors declare that they have no known competing financial interests or personal relationships that could have appeared to influence the work reported in this paper.

Data availability

Data will be made available on request.

Acknowledgments

The authors acknowledge the support of QNRF through project NPRP13S-0126-200172 (Additive Manufacturing of Mg-Based Porous Tissue Scaffolds) and the contributions of the Qatar Energy and Environmental Research Institute (QEERI) and HBKU core labs for the support provided in the characterization of the samples. The Open Access funding is provided by the Qatar National Library.

Appendix A. Supplementary data

Supplementary data to this article can be found online at https://doi.org/10.1016/j.bprint.2023.e00302.

References

[1] A. al Rashid, S.A. Khan, S.G. Al-ghamdi, M. Koc, Additive manufacturing of polymer nanocomposites : needs and challenges in materials , processes , and applications, J. Mater. Res. Technol. 14 (2021) 910–941, https://doi.org/10.1016/j.jmrt.2021.07.016.

[2] F. Ali, S.N. Kalva, M. Koç, Additive manufacturing of polymer/Mg-based composites for porous tissue scaffolds, Polymers 14 (24) (2022), https://doi.org/10.3390/polym14245460.

[3] P.K. Penumakala, J. Santo, A. Thomas, A critical review on the fused deposition modeling of thermoplastic polymer composites, Compos. B Eng. 201 (2020), 108336, https://doi.org/10.1016/j.compositesb.2020.108336.

[4] D. Rahmatabadi, I. Ghasemi, M. Baniassadi, K. Abrinia, M. Baghani, 3D printing of PLA-TPU with different component ratios: fracture toughness, mechanical properties, and morphology, J. Mater. Res. Technol. 21 (2022) 3970–3981, https://doi.org/10.1016/j.jmrt.2022.11.024.

[5] D. Rahmatabadi, I. Ghasemi, M. Baniassadi, K. Abrinia, M. Baghani, 3D printing of PLA-TPU with different component ratios: fracture toughness, mechanical properties, and morphology, J. Mater. Res. Technol. 21 (2022) 3970–3981, https://doi.org/10.1016/j.jmrt.2022.11.024.

[6] L. Chaunier, S. Guessasma, S. Belhabib, G. della Valle, D. Lourdin, E. Leroy, Material extrusion of plant biopolymers: opportunities & challenges for 3D printing, Addit. Manuf. 21 (2018) 220–233, https://doi.org/10.1016/j.addma.2018.03.016.

[7] H. Lee, et al., Antibacterial PLA/Mg composite with enhanced mechanical and biological performance for biodegradable orthopedic implants, Biomater. Adv. 152 (2023), 213523, https://doi.org/10.1016/j.bioadv.2023.213523.

[8] L.E. Freed, et al., Biodegradable polymer scaffolds for tissue engineering, Bio/Technology 12 (7) (1994) 689–693, https://doi.org/10.1038/nbt0794-689.

[9] G.S. Hussey, J.L. Dziki, S.F. Badylak, Extracellular matrix-based materials for regenerative medicine, Nat. Rev. Mater. 3 (7) (2018) 159–173, https://doi.org/10.1038/s41578-018-0023-x.

[10] S. Sell, et al., Extracellular matrix regenerated: tissue engineering via electrospun biomimetic nanofibers, Polym. Int. 56 (11) (2007) 1349–1360, https://doi.org/10.1002/pi.2344.

[11] R. Imran, A. al Rashid, M. Koç, Review on computational modeling for the property, process, product and performance (PPPP) characteristics of additively manufactured porous magnesium implants, Bioprinting 28 (2022), e00236, https://doi.org/10.1016/j.bprint.2022.e00236. Dec.

[12] A. Gregor, et al., Designing of PLA scaffolds for bone tissue replacement fabricated by ordinary commercial 3D printer, J. Biol. Eng. 11 (1) (2017), https://doi.org/10.1186/s13036-017-0074-3. Oct.

[13] K.A. Athanasiou, C.M. Agrawal, F.A. Barber, S.S. Burkhart, Orthopaedic applications for PLA-PGA biodegradable polymers, Arthrosc. J. Arthrosc. Relat. Surg. 14 (7) (1998) 726–737, https://doi.org/10.1016/S0749-8063(98)70099-4.

[14] J.M. Anderson, M.S. Shive, Biodegradation and biocompatibility of PLA and PLGA microspheres, Adv. Drug Deliv. Rev. 28 (1) (1997) 5–24, https://doi.org/10.1016/S0169-409X(97)00048-3.

[15] K.-J. Chen, F.-Y. Hung, Y.-T. Wang, C.-W. Yen, Mechanical properties and biomedical application characteristics of degradable polylactic acid–Mg–Ca3(PO4)2 three-phase composite, J. Mech. Behav. Biomed. Mater. 125 (2022), 104949, https://doi.org/10.1016/j.jmbbm.2021.104949.

[16] D. Bairagi, S. Mandal, A comprehensive review on biocompatible Mg-based alloys as temporary orthopaedic implants: current status, challenges, and future prospects, National Engg. Reaserch Center for Magnesium Alloys, J. Magnesium Alloys 10 (3) (2022) 627–669, https://doi.org/10.1016/j.jma.2021.09.005. Mar. 01.

[17] V. Tsakiris, C. Tardei, F.M. Clicinschi, Biodegradable Mg alloys for orthopedic implants – a review, National Engg. Reaserch Center for Magnesium Alloys, J. Magnesium Alloys 9 (6) (2021) 1884–1905, https://doi.org/10.1016/j.jma.2021.06.024. Nov. 15.

[18] M. Zeynivandnejad, M. Moradi, A. Sadeghi, Mechanical, physical, and degradation properties of 3D printed PLA + Mg composites, J. Manuf. Process. 101 (2023) 234–244, https://doi.org/10.1016/j.jmapro.2023.05.099.

[19] S.N. Kalva, F. Ali, C.A. Velasquez, M. Koç, 3D-Printable PLA/Mg composite filaments for potential bone tissue engineering applications, Polymers 15 (11) (2023), https://doi.org/10.3390/polym15112572.

[20] F. Ali, A. Al Rashid, S. Kalva, M. Koc, 3D Bioprinting of Mg-Doped PLA Composite as a Potential Material for Bone Tissue Regeneration-Synthesis, Characterization and Additive Manufacturing, 2023, https://doi.org/10.21203/rs.3.rs-2816895/v1.

[21] H. Ikram, A. al Rashid, M. Koç, Synthesis and characterization of hematite (α-Fe2O3) reinforced polylactic acid (PLA) nanocomposites for biomedical applications, Composites Part C: Open Access 9 (Oct) (2022), https://doi.org/10.1016/j.jcomc.2022.100331.

[22] M. A, F.H. N.M, A.S. Jamadon Nashrah Hani, Ahmad, Mechanical properties of injection-molded poly-lactic acid (PLA) reinforced with magnesium hydroxide for biomedical application, in: M, R.J. A, M.P.J. Emamian Seyed Sattar, Awang (Eds.), Advances in Material Science and Engineering, Springer Nature Singapore, Singapore, 2023, pp. 363–370.

[23] D. Xu, Z. Xu, L. Cheng, X. Gao, J. Sun, L. Chen, Improvement of the mechanical properties and osteogenic activity of 3D-printed polylactic acid porous scaffolds by nano-hydroxyapatite and nano-magnesium oxide, Heliyon 8 (6) (2022), e09748, https://doi.org/10.1016/j.heliyon.2022.e09748.

[24] S.-Y. Fu, X.-Q. Feng, B. Lauke, Y.-W. Mai, Effects of particle size, particle/matrix interface adhesion and particle loading on mechanical properties of particulate–polymer composites, Compos. B Eng. 39 (6) (2008) 933–961, https://doi.org/10.1016/j.compositesb.2008.01.002.

[25] H. Gollwitzer, et al., Biomechanical and allergological characteristics of a biodegradable poly(D,L-lactic acid) coating for orthopaedic implants, J. Orthop. Res. 23 (4) (2005) 802–809, https://doi.org/10.1016/j.orthres.2005.02.003.

[26] X. Li, Y. Wang, C. Chu, L. Han, J. Bai, F. Xue, A study on Mg wires/poly-lactic acid composite degradation under dynamic compression and bending load for implant applications, J. Mech. Behav. Biomed. Mater. 105 (2020), 103707, https://doi.org/10.1016/j.jmbbm.2020.103707.

[27] T. Motoyama, T. Tsukegi, Y. Shirai, H. Nishida, T. Endo, Effects of MgO catalyst on depolymerization of poly-l-lactic acid to l,l-lactide, Polym. Degrad. Stabil. 92 (7) (2007) 1350–1358, https://doi.org/10.1016/j.polymdegradstab.2007.03.014.

[28] A. Ferrández-Montero, et al., Development of biocompatible and fully bioabsorbable PLA/Mg films for tissue regeneration applications, Acta Biomater. 98 (2019) 114–124, https://doi.org/10.1016/j.actbio.2019.05.026.

[29] M. Mohammadi Zerankeshi, S.S. Sayedain, M. Tavangarifard, R. Alizadeh, Developing a novel technique for the fabrication of PLA-graphite composite filaments using FDM 3D printing process, Ceram. Int. 48 (21) (2022) 31850–31858, https://doi.org/10.1016/j.ceramint.2022.07.117.

[30] J. Lee, et al., Fabrication of poly(lactic acid)/Ti composite scaffolds with enhanced mechanical properties and biocompatibility via fused filament fabrication (FFF)–based 3D printing, Addit. Manuf. 30 (2019), 100883, https://doi.org/10.1016/j.addma.2019.100883.

[31] I. Antoniac, D. Popescu, A. Zapciu, A. Antoniac, F. Miculescu, H. Moldovan, Magnesium filled polylactic acid (PLA) material for filament based 3D printing, Materials 12 (5) (2019), https://doi.org/10.3390/ma12050719.

[32] S.C. Cifuentes, R. Gavilán, M. Lieblich, R. Benavente, J.L. González-Carrasco, In vitro degradation of biodegradable polylactic acid/magnesium composites: relevance of Mg particle shape, Acta Biomater. 32 (2016) 348–357, https://doi.org/10.1016/j.actbio.2015.12.037.

[33] C. Shuai, Y. Li, P. Feng, W. Guo, W. Yang, S. Peng, Positive feedback effects of Mg on the hydrolysis of poly-l-lactic acid (PLLA): promoted degradation of PLLA scaffolds, Polym. Test. 68 (2018) 27–33, https://doi.org/10.1016/j.polymertesting.2018.03.042.

[34] G.L. Song, A. Atrens, Corrosion mechanisms of magnesium alloys, Wiley-VCH Verlag, Adv. Eng. Mater. 1 (1) (1999) 11–33, https://doi.org/10.1002/(SICI)1527-2648(199909)1:1<11::AID-ADEM11>3.0.CO;2-N.

[35] A. Ferrández-Montero, M. Lieblich, R. Benavente, J.L. González-Carrasco, B. Ferrari, Study of the matrix-filler interface in PLA/Mg composites manufactured by Material Extrusion using a colloidal feedstock, Addit. Manuf. 33 (2020), 101142, https://doi.org/10.1016/j.addma.2020.101142.

[36] J.O. Akindoyo, M.D.H. Beg, S. Ghazali, H.P. Heim, M. Feldmann, Effects of surface modification on dispersion, mechanical, thermal and dynamic mechanical properties of injection molded PLA-hydroxyapatite composites, Compos Part A Appl Sci Manuf 103 (2017) 96–105, https://doi.org/10.1016/j.compositesa.2017.09.013.

[37] M. Asadollahi, et al., Improving mechanical properties and biocompatibility of 3D printed PLA by the addition of PEG and titanium particles, using a novel incorporation method, Bioprinting 27 (2022), e00228, https://doi.org/10.1016/j.bprint.2022.e00228.

[38] R. Bakhshi, M. Mohammadi-Zerankeshi, M. Mehrabi-Dehdezi, R. Alizadeh, S. Labbaf, P. Abachi, Additive manufacturing of PLA-Mg composite scaffolds for hard tissue engineering applications, J. Mech. Behav. Biomed. Mater. 138 (2023), 105655, https://doi.org/10.1016/j.jmbbm.2023.105655.